PERGAMON

Vision Research 39 (1999) 3267–3285

Vision Research

www.elsevier.com/locate/visres

Velocity tuned mechanisms in human motion processing

Tobias E. Reisbeck, Karl R. Gegenfurtner *

Max-Planck-Institut für biologische Kybernetik, Spemannstrasse 38, 72076 Tübingen, Germany

Received 6 April 1998; received in revised form 13 October 1998

Abstract

We determined two-dimensional motion discrimination contours in the spatio-temporal frequency plane to characterize the mechanisms underlying velocity perception. In particular, we wanted to determine whether there exist mechanisms tuned specifically to velocity, rather than separable mechanisms tuned to spatial and temporal frequency. A 4-AFC paradigm was used to determine spatio-temporal frequency discrimination thresholds for moving sinewave gratings defined by luminance contrast. Three of the grating patches used were defined by the same spatial and temporal frequency (standard), the other (test) differed by a fixed proportional change in spatial and temporal frequency. Subjects had to indicate which grating differed most from the others and the thresholds determined for varying proportions of change in spatial and temporal frequency were used to trace out complete threshold contours in the plane spanned by these attributes. Some of the contours, primarily at speeds above 1 deg/s, were noticeably oriented along lines of constant velocity. To further isolate these mechanisms, spatio-temporal noise was added to the standard stimuli either along a line of constant velocity or in the direction orthogonal to it. When spatio-temporal noise of constant velocity was added to the standard stimuli, threshold contours became elongated only along the direction of the noise. The same amount of noise in the orthogonal direction produced an overall increase in thresholds without changing the shape of the contour, presenting clear evidence for velocity tuned mechanisms. In further experiments we discovered that velocity tuned mechanisms interact with separable mechanisms to produce optimal discriminability. Analogous experiments with isoluminant stimuli failed to exhibit evidence for velocity tuning, supporting the notion that the human color vision system is impaired in its coding of stimulus speed, despite excellent sensitivity to direction of motion.

Keywords: Motion perception; Spatio-temporal separability; Velocity tuning; Isoluminance; Noise; Contrast

1. Introduction

Research on motion perception has produced important insights at the psychophysical, computational, and neurophysiological level. The activity of individual neurons in the middle temporal area (MT) of macaque monkeys has been closely linked to perceptual performance in direction-of-motion discrimination tasks (Newsome, Britten & Movshon, 1989; Newsome, Britten, Salzman & Movshon, 1990; Salzman, Britten & Newsome, 1990; Britten, Shadlen, Newsome & Movshon, 1992a,b; Salzman, Murasugi, Britten & Newsome, 1992; Britten, Newsome, Shadlen, Celebrini & Movshon, 1996; Newsome, 1997). Furthermore, there are several similar models of motion sensing that closely resemble the underlying neural circuitry and make accurate predictions of psychophysical performance (Reichardt, 1961; Van Santen & Sperling, 1984; Adelson & Bergen, 1985; Watson & Ahumada, 1985; Heeger, 1987; Grzywacz & Yuille, 1990; Smith & Edgar 1994; Heeger, Simoncelli & Movshon, 1996). However, most research has concentrated on the estimation of direction of motion. In contrast, the mechanisms responsible for the computation of object speed are still largely unknown.

The elementary components of all motion models are receptive fields selectively responsive to spatial and temporal frequency (Hubel & Wiesel, 1962; Campbell, Cleland, Cooper & Enroth-Cugell, 1968; Hubel & Wiesel, 1968; Campbell, Cooper & Enroth-Cugell, 1969; Tolhurst & Movshon, 1975; Movshon, Thompson & Tolhurst, 1978a,b,c; De Valois, Albrecht & Thorell, 1982; De Valois & De Valois, 1988). The

* Corresponding author. Tel.: +49-7071-601607; fax: +49-7071-601616.

E-mail address: karl.gegenfurtner@tuebingen.mpg.de (K.R. Gegenfurtner)

0042-6989/99/$ - see front matter
PII: S0042-6989(99)00017-6

outputs of these spatio-temporal filters are then combined, either through correlation or through quadrature, to construct mechanisms that respond to one direction of motion, independently of stimulus contrast or polarity. Since the components of these motion detectors are receptive fields independently tuned to spatial and temporal frequency, the detectors as a whole are also separable in space and time along their preferred direction of motion. That is, the response at any velocity is the product of the response at the spatial and the temporal frequency of the stimulus. Receptive fields with properties mimicking the behavior of these elementary motion detectors (EMDs) have been observed in layer 4B of area V1 (Hubel & Wiesel, 1968; Dow, 1974; Livingstone & Hubel, 1984; Orban, Kennedy & Bullier, 1986; Hawken, Parker & Lund, 1988) and most frequently in area MT (Dubner & Zeki, 1971; Newsome, Gizzi & Movshon, 1983; Albright, 1984; Movshon, Newsome, Gizzi & Levitt, 1988; Britten et al., 1992a,b).

Since the EMDs respond only over the part of the spatio-temporal frequency domain to which its low level receptive fields are tuned to, it is possible in theory to recover stimulus velocity through the simply relationship $v = tf/sf$, i.e. velocity is the ratio of temporal and spatial frequency. That approach is used in several of the common models (Watson & Ahumada, 1985; Heeger, 1987; Heeger et al., 1996; Simoncelli & Heeger, 1998). The question remains whether such velocity tuned mechanisms specifically exist in the human visual system. There is indirect psychophysical evidence pointing towards the existence of velocity tuned mechanisms (McKee, Silverman & Nakayama, 1986). Our goal in the present experiments was to characterize the tuning of these mechanisms, to see how they are distributed over different velocities, whether they are contrast-independent, and whether similar mechanisms exist for the chromatic channels.

Numerous physiological studies have shown that cells in cat and monkey visual cortex can be tuned to velocity (Ikeda & Wright, 1975; Movshon, 1975; Holub & Morton-Gibson, 1981; Orban, Kennedy & Maes, 1981; Maunsell & Van Essen, 1983; Bisti, Carmignoto, Galli & Maffei 1985; Burkhalter & Van Essen, 1986; Morrone, Di Stefano & Burr, 1986; Orban et al., 1986; Movshon et al., 1988). However, in most of these experiments broadband stimuli such as random dot kinematograms have been used, which do not allow to distinguish between velocity tuned and space–time separable mechanisms. We will pursue this issue further in Section 6 of this paper. In the few experiments where sinusoidal grating stimuli were used, no evidence for velocity tuning could be found for neurons in macaque areas V2 or MT (Newsome et al., 1983; Foster, Gaska, Nagler & Pollen, 1985; Movshon et al., 1988; Levitt, Kiper & Movshon, 1994).

Psychophysically, McKee et al. (1986) showed that velocity discrimination was not much affected by random changes in the temporal frequency of moving sinusoidal gratings. They concluded that velocity is the primary source of information for motion discrimination and that temporal frequency has to be derived from velocity. However, later experiments by Smith and Edgar (1991) showed that temporal frequency discriminations are also affected very little by random changes in velocity. Therefore, the two quantities seem to be processed rather independently of each other.

We performed a direct test for separability suggested by McKee et al. (1986). In our initial experiment, we determined discrimination threshold contours in the spatio-temporal frequency plane to test whether the resulting contours could be described as the product of independent mechanisms tuned to spatial and temporal frequency. This type of analysis has been used extensively in the past to determine the mechanisms underlying color discrimination (Nielsen & Wandell, 1988; Poirson, Wandell, Varner & Brainard, 1990; Krauskopf & Gegenfurtner, 1992; Gegenfurtner & Hawken, 1995).

Since the results of measuring discrimination contours were not entirely conclusive, we performed further experiments using noise masking techniques that have been successfully used in the past to isolate mechanisms of spatial vision (Henning, Hertz & Hinton, 1981; Pelli, 1981; Wilson, McFarlane & Phillips, 1983; Legge, Kersten & Burgess, 1987; Derrington & Henning, 1989) and color vision (Switkes, Bradley & De Valois, 1988; D'Zmura, 1990; Gegenfurtner & Kiper, 1992; Losada & Mullen, 1994, 1995; Sankeralli & Mullen, 1997). The noise masking experiments provide conclusive evidence that velocity tuned mechanisms exist in the human visual system. However, under normal circumstances velocity tuned mechanisms seem to act together with space–time separable mechanisms. We performed a third experiment in which we determined psychometric functions for different directions in the spatio-temporal frequency plane to investigate the possible interactions between the three mechanisms more thoroughly.

Finally, we repeated the whole series of experiments using stimuli defined exclusively by color contrast (isoluminant stimuli). Under these conditions no evidence for velocity tuning was found, which further supports the notion that the perception of stimulus speed is severely impaired at isoluminance (Cavanagh, Tyler & Favreau, 1984; Mullen & Boulton, 1992; Teller & Lindsey, 1993; Hawken, Gegenfurtner & Tang, 1994; Gegenfurtner & Hawken, 1996a), despite an excellent sensitivity of the human color vision system to direction of motion (Stromeyer, Eskew & Kronauer, 1990; Cavanagh & Anstis, 1991; Derrington & Henning, 1993; Metha, Vingrys & Badcock, 1994; Stromeyer, Kronauer, Ryu, Chaparro & Eskew, 1995; Gegenfurtner & Hawken, 1996b).

Preliminary reports of these data have been presented in Reisbeck and Gegenfurtner (1997).

2. Experiment 1: Threshold contours in the spatiotemporal frequency plane

Discrimination thresholds were measured in the two-dimensional space spanned by spatial and temporal frequency. For a certain standard stimulus (drifiting sinusoidal gratings) of a given spatial and temporal frequency, we determined the just noticeable difference at which a test stimulus in a certain direction away from the standard could be reliably discriminated. Standard stimuli covered a range of velocities from about 0.05 up to about 15 deg/s. Fig. 1 illustrates the potential outcomes of such an experiment. If the mechanisms of motion discrimination are space–time separable, then we would expect discrimination contours that are aligned to the axes of the spatio-temporal frequency plane, as in Fig. 1A. If velocity tuned mechanisms exist, we would expect the discrimination contours to be aligned along lines of constant velocities through the standard stimuli, as in Fig. 1B. This plot also shows how such a velocity tuned mechanism might be built by pooling lower-level space–time separable mechanisms.

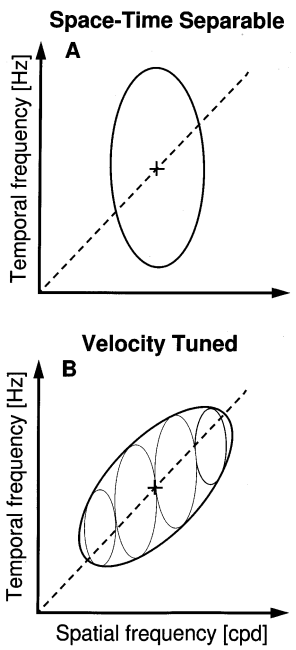

Fig. 1. Mechanisms responsible for the processing of stimulus velocity. The abscissa of each plot denotes spatial and the ordinate temporal frequency. The broken lines indicate locations of equal velocity which are given by the slopes of the lines, e.g. the ratio of temporal to spatial frequency. The crosses mark the centers of hypothetical receptive fields for a space–time separable (A) and a velocity tuned mechanism (B). Space–time separable mechanisms are realized by receptive fields of cells in V1 of macaque monkeys (heavy ellipse) and cover a certain area in this spatio-temporal frequency plane. The important point is that the optimal spatial frequency of such a cell is independent of the temporal frequency of the presented stimulus and vice versa, e.g. the receptive field's main axes are aligned with the coordinate axes. To construct a velocity tuned mechanism as the one presented in B (heavy ellipse) at a later processing stage, information from cells of the former stage that are tuned to the same velocity (thin ellipses) has to be combined. In this case the contour of the receptive field is tilted with respect to the coordinate axes. Therefore, the maximal activation of the cell is only elicited for covarying spatial and temporal frequencies such that the formula $v = tf/sf$ holds. Maximal activation depends on the velocity of the stimulus that is being processed.

2.1. Methods

2.1.1. Equipment

The stimuli were displayed on a BARCO (CCID 7351B) color television monitor that was driven by a Cambridge Research VSG 2/3 graphics board with a refresh rate of 120 Hz non-interlaced. The images were generated on the monitor by reading through the picture memory in a raster scan and then interpreting the numbers in each location as a color defined in a 256-element color lookup table. Two 8-bit-digital-to-analog converters, which were combined to produce an intensity resolution of 12 bits, were used to control the intensity of each of the three monitor primaries. The luminances of each of the phosphors was measured at various output voltage levels using a Graseby Optronics Model 370 optometer with a model 265 photometric filter. A smooth function was used to interpolate between the measured points and lookup tables were generated to linearize the relationship between voltage output and luminance. All the stimuli in the present experiments had a space–time averaged luminance of 26.25 cd/m^2. We also made sure that additivity of the three phosphors held over the range of intensities used in these experiments (Brainard, 1989). A Photo Research PR 650 spectroradiometer was used to measure the spectra of the red, green and blue phosphor at their maximum intensity setting. The spectra were multiplied with Judd's 1951 color matching functions to derive x, y chromaticity coordinates and the luminance Y of the phosphors (Irtel, 1992). The resulting (x, y, Y) phosphor coordinates were red = (0.61, 0.35, 16.34); green = (0.28, 0.60, 35.96); blue = (0.16, 0.07, 4.86). All further references to luminance and photometric luminance refer to the $V(\lambda)$ curve as modified by Judd. The matrix equations given by MacLeod and Boynton (1979) were used to calculate cone absorptions (Smith & Pokorny, 1975) from the X, Y, and Z values.

2.1.2. Procedure

Subjects were seated at a distance of 172 cm from the monitor. Their heads were resting on a chin rest and they viewed the scene binocularly through natural pupils. At a distance of 65 cm from the monitor a panel 200×200 cm in size with an aperture of 20×15 cm

was placed in the frontoparallel plane. The area that was visible on the screen therefore subtended $10.7 \times 8°$ of visual angle. The panel and the monitor were connected by a tube of 50×40 cm side length. In this way no illuminating light from above could reach the monitor screen on a direct path. Its interior was coated with black felt such that there was no reflection of light entering the tube. The color of the panel was chosen to match the monitor screen both with respect to the uniform gray background color and its mean luminance of 26.25 cd/m^2. This was done to give the impression of a continuous screen on which the stimuli were presented. At the center of the monitor a black fixation square of 8 min side length was displayed.

2.1.3. Subjects

Three subjects (TR, SH, KL), one of which was the first author (TR), participated in the first experiment. All subjects had normal or corrected to normal visual acuity and normal color vision.

2.1.4. Stimuli

The stimuli in Experiment 1 were vertically oriented drifting sinewave gratings of different spatial and temporal frequencies, defined by luminance contrast. We used a 4-AFC paradigm to determine discrimination thresholds in the spatio-temporal frequency plane for sinewave gratings defined by 50% luminance contrast. Configuration of the stimuli can be seen in Fig. 2A.

The stimuli consisted of four discs each 1° in diameter. The centers of the discs were located 1.06° eccentric on the corners of an imaginary square that was symmetrically arranged around the fixation spot. During each presentation three of the discs showed the same sinewave gratings (standard stimuli) and the fourth showed a grating that differed in spatial frequency, temporal frequency or simultaneously in both stimulus attributes (test stimulus in Fig. 2A: lower left). For 16 test directions, which differed by the proportion of change in spatial and temporal frequency with respect to the standard, we determined the just noticeable differences. These directions are depicted by the arrows in Fig. 2B, where the location of the standard stimulus is represented by the cross in the center of the plot. The starting spatial phase was randomly chosen for each grating and during each trial all stimuli moved randomly either to the left or to the right. Presentation time was 500 ms and stimulus contrast was ramped on and off during the first and last 50 ms. Subjects had to indicate which one of the discs was different from the others. They did so by pressing one of four keypad buttons representing the locations of the discs on the screen. An adaptive staircase procedure defined by an up-down method (Levitt, 1971) controlled the magnitude of the difference between standard and test stimuli. The difference between the test and standard stimuli was decreased after three consecutive correct responses and increased after an incorrect response. Threshold estimates were then determined from the mean of the six reversal points of the staircase. This was done at least three times for each of the different directions. The average values of these measurements were used as the final estimates for the thresholds. The 16 individual thresholds were used to trace out a complete two-dimensional threshold contour in the spatio-temporal frequency plane. For observer TR, 14 threshold contours were determined which covered a range of spatial frequencies from 0.5 to 8 c/deg and a range of temporal frequencies from 0.5 to 8 Hz. For the other observers only seven or five threshold contours were determined, thereby covering the same range of temporal but a smaller range of spatial frequencies (0.5–4 c/deg).

2.2. Results

Fig. 3 shows the threshold contours for subjects TR, SH and KL. We determined 14 (subject TR), seven (subject SH) or five (subject KL) threshold contours for the standard stimuli given by the crosses in the different plots. The lines of constant velocity, which all run through the origin in a linear plot, are parallel at 45° in this log–log plot. This makes it easier to evaluate the orientation of the ellipse for speeds that are represented close to the axes. The abscissas denote spatial frequency and the ordinates temporal frequency. The closed curves through the data points are the best fitting ellipses. The methods used for the fitting are described in great detail in Gegenfurtner and Hawken (1995).

Over a range of spatial and temporal frequencies, the size of the threshold contours is fairly constant in this log–log plot. This means that, as expected from predictions of Weber's law for spatial and temporal frequency discriminations, threshold contours became larger with increasing spatial or temporal frequency. Additionally, many of the contours are severely tilted away from the axes of the coordinate system. This does not conform with the prediction based on separable mechanisms for spatial and temporal frequency (see Fig. 1A). Rather, the contours are tilted at angles close to 45°. In the linear coordinate system these contours would point towards the origin, indicating non-separable, velocity tuned mechanisms (see Fig. 1B). The quality of the prediction based on velocity tuned mechanisms can be evaluated by looking at the angles the major axes of the ellipses form with the coordinate axes. Velocity tuning predicts that the major axes of all ellipses should be aligned to a line through the origin and the standard stimulus, resulting in an orientation of 45° in the log–log plot shown in Fig. 3. Fig. 4 shows the orientation of the ellipses as a function of the velocity of the standard stimulus. For velocities above 1 deg/s, many of the

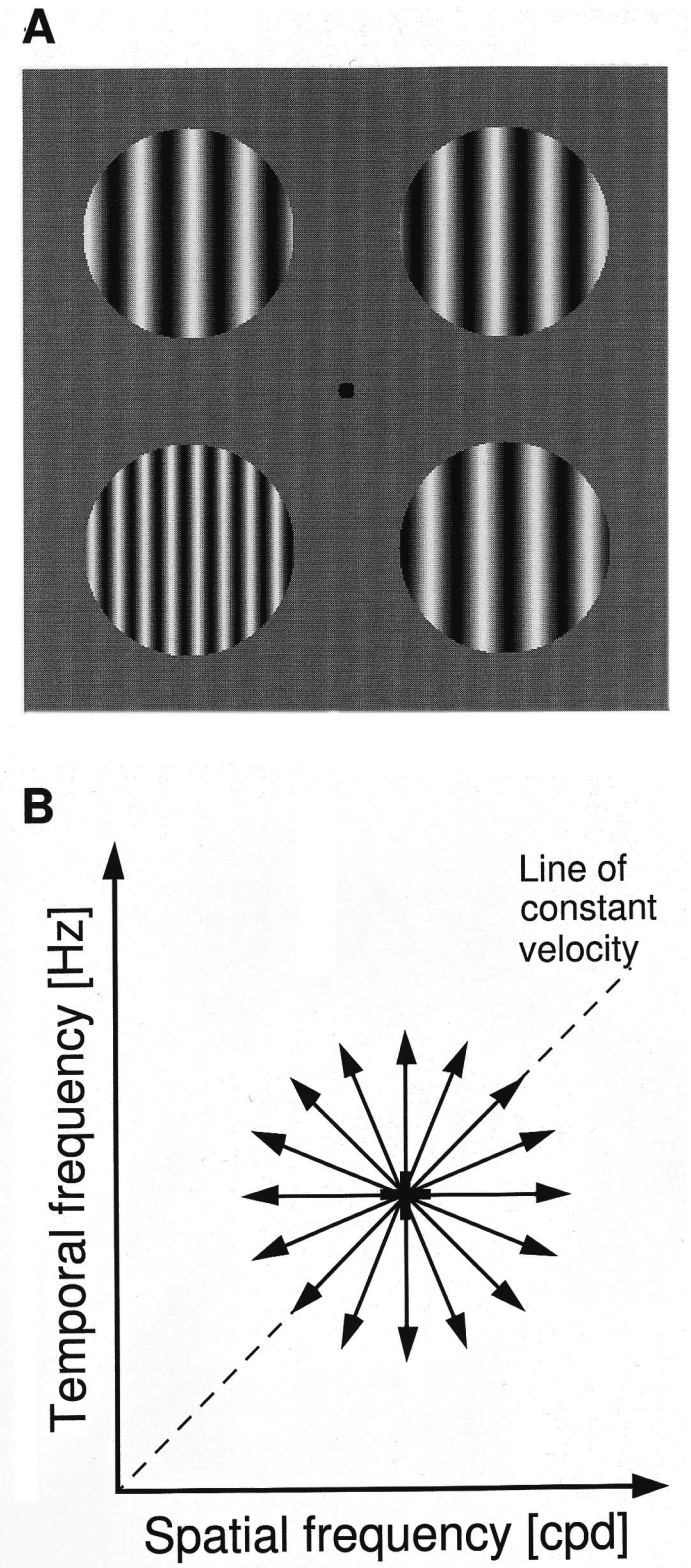

Fig. 2. The paradigm used in Experiment 1 to determine spatio-temporal discrimination contours. (A) We used a 4 AFC-paradigm in which three stimuli were identical (standards) and one (test) differed in spatial frequency, temporal frequency or both. Subjects had to indicate the test stimulus (lower left) and discrimination thresholds were determined using an adaptive staircase procedure. (B) The plot shows the 16 different test directions away from the standard stimulus (cross) for each of which the proportion of change in spatial and temporal frequency was different. The broken line indicates locations of constant velocity.

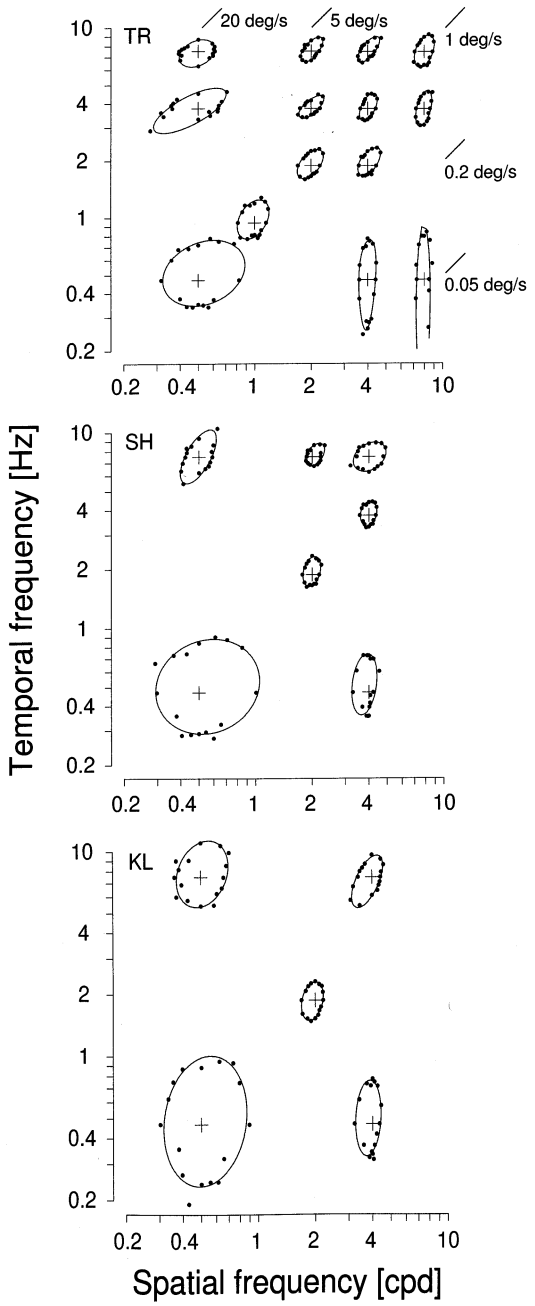

Fig. 3. Threshold contours in the spatio-temporal frequency plane for three observers (TR, SH and KL). Axes are plotted on a logarithmic scale where the abscissa denotes spatial and the ordinate temporal frequency of the stimulus gratings. The crosses in each plot mark the location of the standard gratings. The lines above and on the right hand side of the upper plot indicate directions of constant velocities which are given next to them. Thresholds are represented by the filled circles for 16 different test directions away from the standard stimulus. The smooth contours through the data points show the best fitting ellipses. Those threshold contours that are tilted with respect to the coordinate axes indicate that velocity tuned mechanisms contribute to the discrimination performance of the subjects in this experiment.

ellipses are oriented close to 45°, indicating velocity tuned mechanisms. At the slowest speeds, the ellipses tend to be oriented close to 90°, in line with the prediction based on separable mechanisms.

One natural explanation for the separability at the slowest speeds would be the absence or missing sensitivity at slow speeds. This would be in line with the observed contrast dependence at slow speeds (Thompson, 1982; Stone & Thompson, 1992; Hawken et al., 1994). However, another possibility that cannot be excluded is given by the space–time localized nature of the stimuli. Since the stimuli are windowed by a ramp in time and by a step in space, they are not strictly points in the frequency diagrams (such as Fig. 3). Rather, the Fourier energy is spread out along the spatial and temporal frequency domains. Even though any such spread is strictly separable in spatial and temporal frequency, the relative spread will be larger for stimuli with low temporal and low spatial frequencies, and as such could serve to mask the possible influence of velocity tuned mechanisms. At higher spatial and temporal frequencies the effect of the spread becomes negligible.

Fitting ellipses amounts to finding a linear transformation of the coordinate space which transforms the ellipse into a unit circle. Since we found small asymmetries in the detection of increments and decrements in some cases, we allowed the center of the ellipse to vary as well. The quality of the ellipse fit can then be determined by calculating the deviations of the transformed points from the unit circle (Poirson et al., 1990). These deviations, for the data shown in Fig. 3, ranged from 0.2 up to 2.2% with a mean of 0.8%. This can be considered an excellent fit, especially when compared to typical goodness-of-fit values of around 5% obtained in

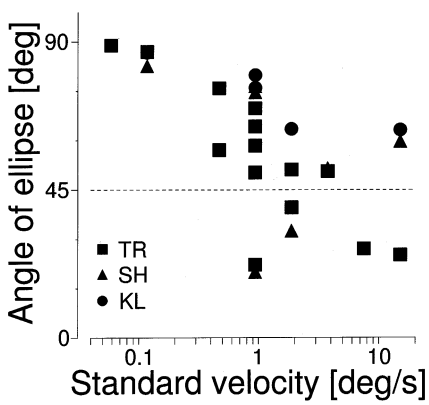

Fig. 4. The orientation of the best fitting ellipses (see Fig. 3) as a function of the velocity of the different standard gratings. Subjects are indicated by their initials in the lower left hand corner of the plot. The abscissa represents the velocity of the standard grating on a logarithmic scale, whereas the ordinate indicates the angle of the best fitting ellipses. The broken horizontal line at 45° indicates the prediction for velocity tuned mechanisms. At high velocities many ellipses are oriented close to 45° indicating that velocity tuned mechanisms mediate discrimination performance. For low velocities the orientations of the best fitting ellipses were close to 90°.

other domains (Nielsen & Wandell, 1988; Poirson et al., 1990; Krauskopf & Gegenfurtner, 1992; Gegenfurtner & Hawken, 1995). In contrast, when we fitted the data with ellipses aligned to the coordinate axes, the average fit was much worse with an average deviation of 4.2%, and a range of deviations between 0.6 and 10.2%. The later fits show clear and systematic deviations of the data from the predictions. We therefore reject the hypothesis that the discrimination contours are solely due to separable mechanisms tuned to spatial and temporal frequency.

2.3. Discussion

The results provide direct evidence for some velocity tuned mechanisms in human visual motion processing. The thresholds shown in Fig. 3 are smallest in directions orthogonal to lines of constant velocity. Presumably, these discriminations are based on the activity of velocity tuned mechanisms. Thresholds are elongated along lines of constant velocity, since velocity tuned mechanisms cannot be used for discrimination along such lines. Discrimination of stimuli of equal velocity has to be based on differences in spatial and temporal frequency. The data in Fig. 3 indicate that the difference in thresholds along directions of constant velocity and of changing velocity are not very dramatic. This implies that mechanisms selective to spatial and temporal frequency might affect at least part of the discrimination contour. We therefore devised a second experiment that would allow us to investigate the velocity tuned mechanism in more detail, without the interference of spatial and temporal mechanisms.

3. Experiment 2: Influence of spatio-temporal noise

A technique widely used to isolate mechanisms underlying certain aspects of spatial vision (Henning et al., 1981; Pelli, 1981; Wilson et al., 1983; Legge et al., 1987; Derrington & Henning, 1989) or color vision (Switkes et al., 1988; D'Zmura, 1990; Gegenfurtner & Kiper, 1992; Losada & Mullen, 1994, 1995; Sankeralli & Mullen, 1997) is noise masking. The basic idea is that adding stimulus noise to a visual channel will decrease its signal-to-noise ratio and therefore the psychophysical detection performance based on this channel will deteriorate. When several mechanisms are at work interactively, noise can be added differentially to each of them, thereby selectively decreasing detection or discrimination thresholds within that channel. By doing so we can expose a larger part of the detection or discrimination contour that depends upon the other mechanisms. Of course, at a more basic level, it also allows an assessment of whether more than one such mechanism is present.

In the experiment described here we added two different types of spatio-temporal noise to the three standard stimuli used in the discrimination task. Noise could be a modulation along a line of constant velocity. That is, we added or subtracted amounts of spatial and temporal frequency to each of the three standards, such that the resulting ratio of temporal to spatial frequency (i.e. velocity) was unchanged. To a velocity tuned mechanism this kind of noise will be invisible. Under a second condition, we used noise with the same magnitude of spatial and temporal frequency modulations, but with reverse signs, as illustrated in Fig. 5. Therefore, the second type of noise will perturb velocity tuned mechanisms in the same way it affects mechanisms tuned to spatial and temporal frequency.

The reasoning behind this experiment was first to strengthen the evidence in favor of the existence of velocity tuned mechanisms, and second to uncover the parts of the threshold contours that are based on velocity tuned mechanisms exclusively.

3.1. Methods

Methods were identical to the ones used in Experiment 1, except that we applied two different kinds of spatio-temporal noise to the standard stimuli, as can be seen in Fig. 5B. The thick bar with positive slope indicates noise along a line of constant velocity. Noise with varying velocity was chosen along a line that resulted from vertically reflecting the line of constant velocity around the location of the standard stimulus. This is indicated by the thick bar with negative slope. Noise was uniformly distributed between the endpoints of these lines. In both experiments, we used the same absolute amount of spatio-temporal noise and its maximal extent equalled twice the noise-free discrimination threshold that was determined in Experiment 1 for the constant velocity direction. Application of noise resulted in three different standard sinewave gratings that were randomly picked from the line of constant (first condition, bar with positive slope) or variable velocity (second condition, bar with negative slope). Under both conditions the spatial and temporal frequencies of all stimuli were different. In the first case, however, the standards had the same velocity and the test could therefore be discriminated by its velocity difference. In the second case, the velocity also varied for all stimuli. Test stimuli were again chosen along 16 directions around the standard stimulus. The subjects had to indicate the patch which differed most from the others. Fig. 5A shows a typical stimulus configuration with four grating patches all differing in spatial and temporal frequency. Measurements for both types of noise were performed in different experimental sessions, while the individual contours were randomly split up into two consecutive experimental sessions. Threshold contours

for both directions of noise and the condition without noise were determined for five observers, three of whom already participated in the first experiment.

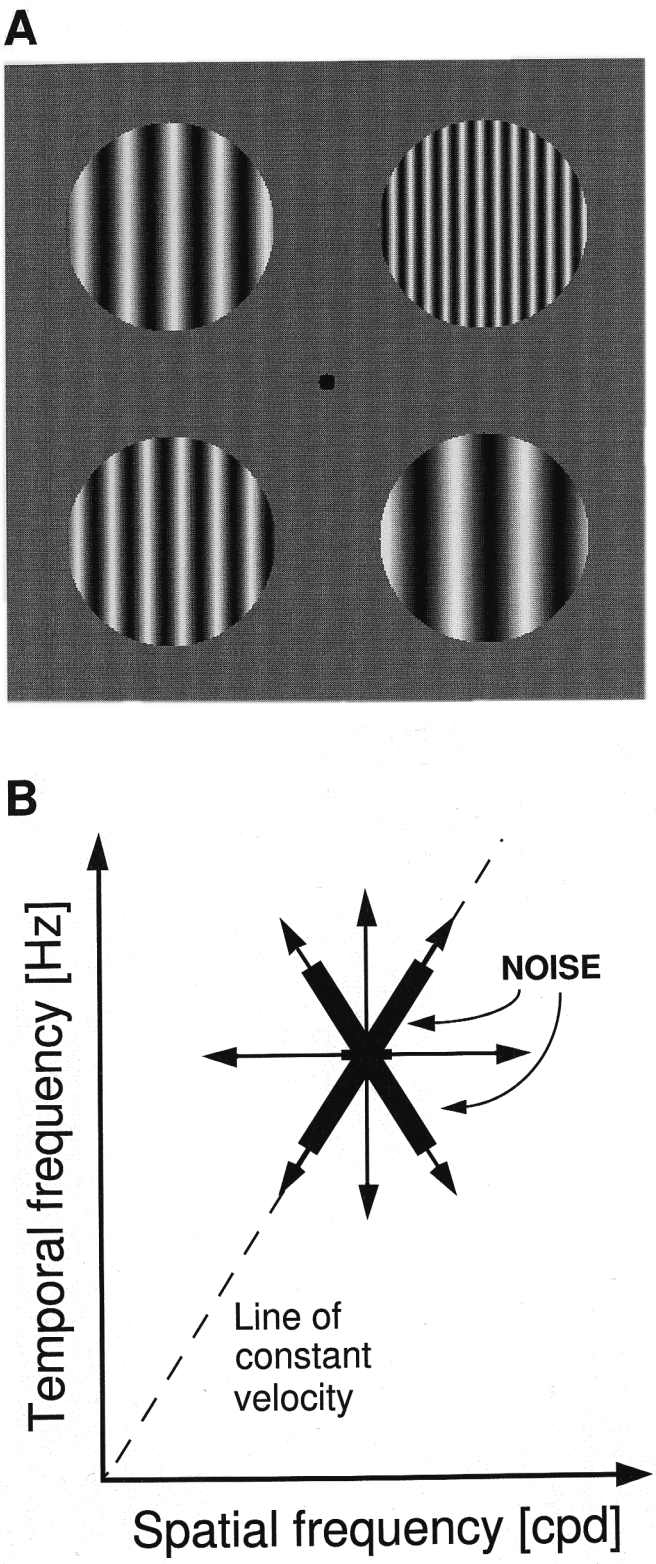

Fig. 5.

3.2. Results

The results for three subjects (TR, KH and DU) are shown in Fig. 6. The results for two other naive observers did not differ in any systematic way. The abscissa of each plot denotes spatial frequency and the ordinate temporal frequency. The cross in the center of each plot shows the location of the standard stimulus which had a spatial frequency of 2 c/deg and a temporal frequency of 1.875 Hz. The small filled diamonds represent the threshold contour that has been determined for this standard in Experiment 1 for the respective subjects.

The upper plots (A–C) show the threshold contours for spatio-temporal noise of constant velocity. The maximal amount of noise is given by the length of the two arrows which lie along a line through the origin. The thresholds that were determined for this condition are given by the filled circles in Fig. 6A–C. The resulting contours show a clear elongation along the constant velocity axis, whereas thresholds increase only slightly for directions of variable velocity. For all subjects the long flanks of the threshold contours lie along lines of constant velocity, indicating that velocity tuned mechanisms form the basis of the subjects' discrimination judgments.

The lower plots (D–F) show the threshold contours for the same subjects when noise was applied along a direction of variable velocity. Again, the maximal amount of noise is given by the two arrows. It is important to note that the same absolute amount of spatial and temporal noise was introduced as in the above condition. The resulting threshold contours are given by the filled squares in Fig. 6D–F. Here, an overall increase of thresholds by a factor of 2–3 occurred as a result of the noise that had been added to the standard stimuli.

3.3. Discussion

These results prove the existence of velocity tuned mechanisms in human motion perception. Furthermore, they clarify the special role played by velocity, since no mechanisms selective to the reverse combina-

Fig. 5. The paradigm used in Experiment 2 to determine spatio-temporal discrimination contours when two kinds of noise were applied. We used the same paradigm as described in Fig. 2. Additionally, either noise of constant or variable velocity was added (B). The added noise was twice the threshold determined from Experiment 1 for the direction of constant velocity. Standard stimuli were picked at random from the regions indicated by the solid bars. In each condition spatial and temporal frequencies were different for all stimuli (A). For noise of constant velocity, however, all standard gratings had same velocity and test stimuli could be discriminated by their velocity difference. For variable velocity noise, all stimuli differed in velocity and the discrimination task (A: upper right) could not use velocity as a cue.

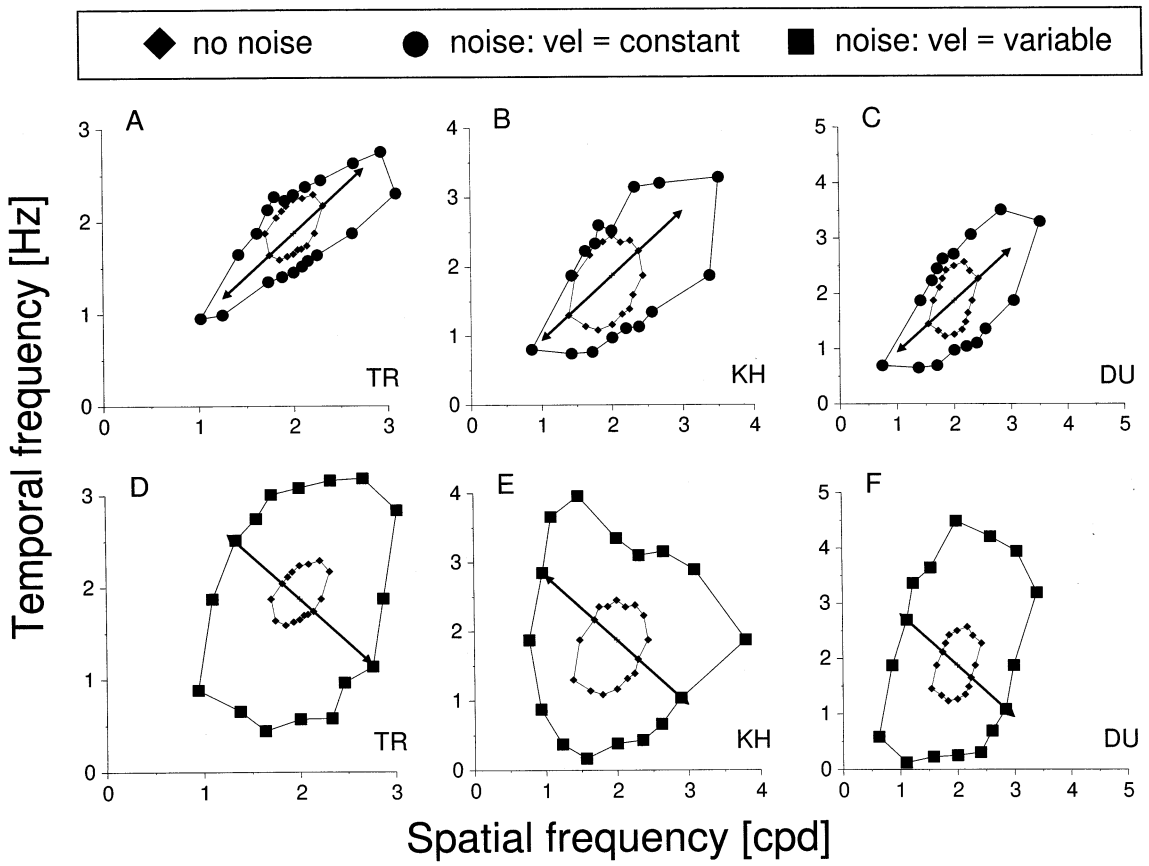

Fig. 6. Spatio-temporal discrimination contours for three subjects (TR, KH and DU) when noise of constant (A–C) or variable velocity (D–F) was added to the standard stimuli. For all subjects the standard stimulus is identical and given by the cross in the center of each plot. Diamonds denote discrimination contours that have been obtained in Experiment 1 without noise. For the constant velocity condition (A–C) discrimination contours are elongated along the constant velocity axis, which is due to the fact that spatiotemporal noise is impairing discrimination based upon spatial and temporal frequency. For other directions information about the velocity of the test stimulus can still be used for discrimination and therefore thresholds increase only slightly. For noise of variable velocity (D–F) discrimination based upon velocity differences is no longer possible. This results in an overall increase in thresholds.

tion of spatial and temporal frequency was found. Selective masking occurred only for noise along the line of constant velocity. This rules out a model with multiple mechanisms distributed evenly across different directions in the spatio-temporal frequency plane. When noise of variable velocity is introduced, all three potential mechanisms are equally affected and thresholds increase uniformly in all directions.

4. Experiment 3: Psychometric functions

The previous two experiments show clear evidence for velocity tuned mechanisms. However, the thresholds determined in these experiments were rather high when compared to conditions of optimal discriminability. The Weber fractions for velocity discrimination thresholds can be as low as 5% (McKee, 1981; McKee & Nakayama, 1984; Orban, De Wolf & Maes, 1984; DeBruyn & Orban, 1988; Snowden & Braddick, 1991). In the previous experiments we observed typical Weber fractions of 10–20%. This was the case, because the conditions used in these experiments were far from ideal. Four patches, presented in the perifovea, had to be monitored at the same time. Changes within each session could be along many different directions in the spatio-temporal frequency plane and comparisons made across different regions of the visual field. We therefore performed a third experiment using a memory matching task that is known to produce highly accurate velocity discrimination (McKee et al., 1986) with optimal Weber fractions. This should allow us to answer the question whether velocity tuned mechanisms contribute to perceptual discriminations of small velocity differences.

4.1. Methods

A method of constant stimuli was used to determine just noticeable differences for simultaneous changes in spatial and temporal frequencies for sinewave gratings

defined by 50 or 6.25% luminance contrast. To measure psychometric functions we determined the proportion of correct responses for 11 test stimuli that were symmetrically placed along each of two directions around the standard stimulus. Each stimulus, including the standard, was presented 80–120 times. The two directions in which comparison stimuli could be placed were chosen in the same way as in Experiment 2. One set of comparison stimuli lay on a line of velocity equal to that of the standard. The other set of points had the same changes in spatial and temporal frequency, but with the reverse polarity (see Fig. 5). Note that the only difference between the two sets is that in the first case the standard and comparison stimuli are of equal velocity, while in the later case there is a velocity difference.

One stimulus patch, 8° in diameter, was presented for 500 ms on each trial. It was oriented vertically and moved randomly to the right or to the left. Between stimulus presentations a fixation square of 8 min side length was displayed at the center of the monitor screen. The experiments consisted of two parts. In the preparatory part the standard stimulus was presented repeatedly to allow subjects to familiarize themselves with it. During the second part, the standard stimulus was presented randomly on 10% of all trials, accompanied by a tone to identify it to the subjects. After presentation of the comparison stimuli, subjects had to decide whether the test stimulus had a higher or lower spatial frequency or moved faster or slower than the standard stimulus, depending on which set of stimuli was tested. They did so by pressing one of two buttons on a keypad. In all experiments the standard stimulus was also used as one of the comparison stimuli. The data points were fitted by a cumulative normal distribution and the standard deviation of the Gaussian was used as a measure of discriminability. Generally, the psychometric functions were centered closely at the standard. The experiments were performed by six observers, five of which already served as subjects in the previous experiments.

4.2. Results

Fig. 7 shows example psychometric functions for three subjects (TR, KL and KH) and three different standard stimuli with 50% luminance contrast. The abscissas denote spatial frequency of the standard and the ordinates the proportion of responses of either higher spatial frequency or higher velocity. Filled circles indicate the proportion of higher spatial frequency/higher temporal frequency responses to stimuli of constant velocity whereas the filled squares represent the proportion of lower spatial frequency/higher temporal frequency (velocity) responses to stimuli of variable velocity. The continuous solid lines are the best fitting psychometric functions to the data points. In all three

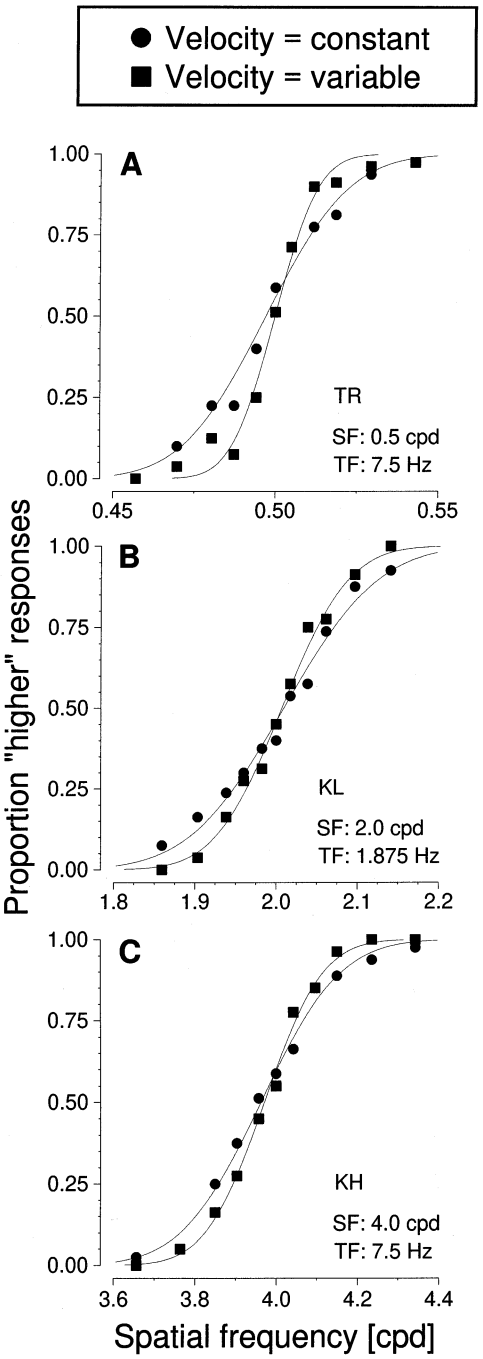

Fig. 7. Psychometric functions for directions of constant and variable velocity for three different observers and standard conditions. The abscissa of each plot depicts spatial frequency and the ordinate the proportion of answers that indicate a higher spatial frequency or velocity than the standard. The respective standard conditions are given in the lower right hand corner of the plot, above them subjects are indicated by the initials. The circles indicate data points determined for the constant velocity direction and the squares those for the direction of variable velocity. The solid lines represent the psychometric functions that have been fitted to the data. They intersect approximately at the spatial frequency of the standard stimulus since standard and test stimuli are identical at this point and discrimination performance is at chance. For each of the plots the psychometric function is steeper for the variable velocity direction indicating lower thresholds and therefore better discrimination performance.

cases the psychometric functions for stimuli of variable velocity are steeper than those for stimuli of constant velocity. For each of the standard conditions indicated in the lower right hand corner of the plots discriminability was higher for stimuli containing an additional velocity component.

Fig. 8 presents the thresholds obtained in this way for 25 (subject TR) or five (subjects KL and NP) different standard stimuli. The abscissas denote spatial frequency and the ordinates represent the temporal frequency of the stimuli. The length of the lines represent the magnitude of discrimination thresholds which are, in this case, five times enlarged for greater visibility. Longer lines correspond to higher thresholds. The lines of positive slope represent thresholds for directions of constant velocity and those with negative slope directions of variable velocity. Their intersections indicate the locations of the standard stimuli. For all standard stimuli the threshold was higher for directions of constant velocity than for directions of variable velocity. The overall increase in thresholds with spatial and temporal frequency is similar to the one observed in Experiment 1, even though it appears different in this linear plot.

Fig. 9A shows a direct comparison of thresholds for directions of variable against directions of constant velocity for stimuli that were characterized by a luminance contrast of 50%. The ratio of thresholds for directions of constant velocity to thresholds for directions of variable velocity is plotted as a function of standard velocity. The broken horizontal line indicates a ratio of 1, the prediction based on spatial and temporal frequency tuned mechanisms alone, i.e. no difference between the two directions. However, all data points do lie above this line thereby indicating that thresholds for directions of variable velocity are generally lower than those for directions of constant velocity. This is the case for all velocities investigated.

Since motion based mechanisms are typically ascribed a high contrast sensitivity (Sclar, Maunsell & Lennie, 1990) we hypothesized that the facilitatory effect of velocity differences might be even larger when stimuli of lower contrast are used. We therefore repeated the above experiment using stimuli of 6.25% luminance contrast. The results are shown in Fig. 9B. In this case we did not observe the advantage for stimuli containing an additional velocity component. Thresholds were equal irrespective of whether a direction of constant velocity or one of variable velocity was tested.

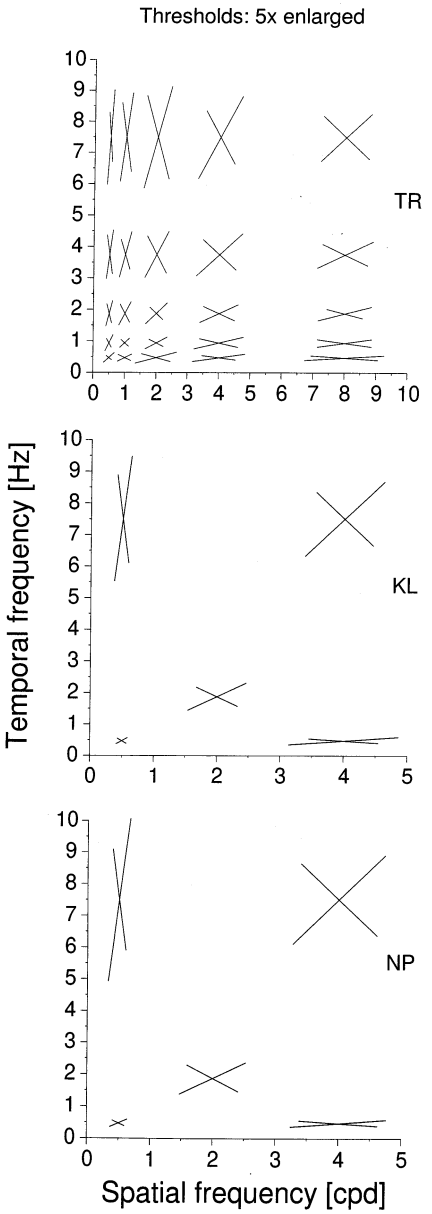

Fig. 8. Discrimination thresholds (× 5) for directions of constant and variable velocity for three subjects. The subjects are indicated by their initials on the right hand side of the plots. The abscissas represent spatial and the ordinates temporal frequency. Using a method of constant stimuli discrimination thresholds have been determined for 25 (TR) or five (KL, NP) standard stimuli. The thresholds are represented by the lines in the directions of constant (positive slope) and variable velocity (negative slope). They intersect at the location of the standard stimulus. The lines of variable velocity (negative slope) are shorter than those for constant velocity (positive slope) indicating better discrimination performance for stimuli along these directions. Note that the discrimination thresholds are enlarged by a factor of 5 for reasons of greater visibility and that the scaling is different for subjects KL and NP.

4.3. Discussion

The conditions in this experiment were chosen to produce optimal velocity discrimination thresholds. Weber fractions in this experiment were generally of the order of 5%. Under these conditions we also found clear evidence that thresholds were at least partly mediated by velocity tuned mechanisms, but only at high

contrasts. This later finding comes as a surprise, since we expected velocity tuned mechanisms to possess the high contrast sensitivity typically ascribed to the motion pathway and especially area MT. However, there is no physiological evidence to date that neurons in area MT are actually tuned to velocity. Preliminary findings reported by two studies (Newsome et al., 1983; Movshon et al., 1988) point to a majority of separable cells in area MT. Therefore, areas higher up in the motion processing hierarchy might be responsible for the extraction of stimulus velocity, and their contrast sensitivity could well be lower than at the preceding stages. These results reiterate the fact that contrast plays an important role in motion processing. They agree with results showing a linear effect of contrast on perceived speed over the whole range of contrasts (Thompson, 1982; Stone & Thompson, 1992; Hawken et al., 1994; Gegenfurtner & Hawken, 1996a). This is vastly different from the results of experiments on the perception of direction of motion, where a saturation is observed at rather modest levels of about 10% contrast (Nakayama & Silverman, 1984), in agreement with an early saturation of MT neurons (Sclar et al., 1990).

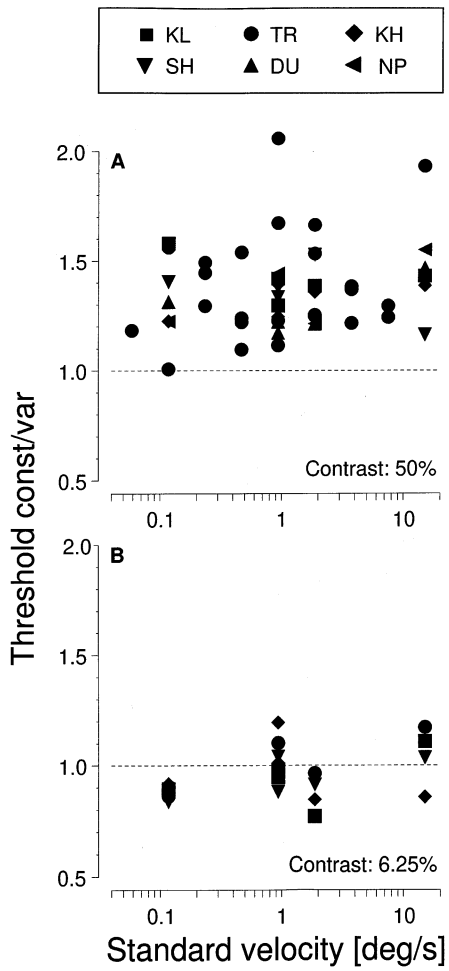

Fig. 9. Ratio of discrimination thresholds for the directions of constant to variable velocity as a function of the velocity of the different standard gratings in Fig. 8. The abscissas represent the velocity of the standard gratings on logarithmic scales and the ordinates the ratio of the thresholds for the two directions. The upper plot (A) shows the data for the six observers who participated in the experiment. Stimuli had a luminance contrast of 50%. The lower plot (B) shows the results for the same observers when stimuli had a luminance contrast of 6.25%. In this case, thresholds were determined for four out of the six observers. The broken horizontal lines in each plot predict the location of the data points if there were no differences in the discrimination performance for the two directions. This, however, is only true for the low contrast gratings. Data points for the high contrast gratings lie above this line indicating that discrimination is better for directions of variable velocity and that velocity tuned mechanisms mediate this superior performance.

5. Experiment 4: Isoluminant gratings

In the recent past, perceived speed has been studied extensively in the context of a possible segregation between motion and color processing (Livingstone & Hubel, 1987). Stimuli defined by chromatic information alone, so called iso- or equi-luminant stimuli, appear to move slower than stimuli defined by luminance (Cavanagh et al., 1984; Mullen & Boulton, 1992; Teller & Lindsey, 1993; Hawken et al., 1994). While this was often interpreted as a general impairment of motion perception at isoluminance, it has been shown recently that the sensitivity for direction of motion is excellent at isoluminance (Stromeyer et al., 1990; Cavanagh & Anstis, 1991; Derrington & Henning, 1993; Metha et al., 1994; Stromeyer et al., 1995; see Gegenfurtner & Hawken, 1996b for a recent review).

The question whether there exist velocity tuned mechanisms for stimuli defined by color only is therefore of interest in further resolving the question of chromatic motion processing. Consequently, we repeated some of the earlier experiments using isoluminant red–green stimuli.

5.1. Methods

Methods were identical to the ones described earlier for Experiments 1 and 3. The same subjects as in Experiment 3 served in this experiment. Now, rather than stimuli defined by luminance contrast we used red–green isoluminant stimuli.

5.1.1. Stimuli

All modulations were symmetric around a neutral white point ($x, y, Y = 0.34, 0.35, 26.25$) along a red–green axis, which was chosen to differentially excite the putative L–M color-opponent mechanism as defined by Krauskopf, Williams and Heeley (1982). The maximum stimulation along the L–M axis went from (0.42, 0.31) to (0.22, 0.39) and produced a Weber contrast of 7.96% in the L-cones and 18.29% in the M-cones. To define

the effectiveness of chromatic stimuli we calculated the root-mean-squared contrast in the L- and M-cones: rms = sqrt [0.5 ($l^2 + m^2$)], where l and m are the Weber contrasts in the L- and M-cones, respectively, calculated using the cone fundamentals proposed by Smith and Pokorny (1975). The maximally achievable RMS-cone-contrast under conditions of photometric isoluminance was 14.1%.

5.1.2. Isoluminance

Six observers participated in these experiments. Some of the observers (TR, KL and DU) had already participated in a different set of experiments on orientation discrimination at isoluminance (Reisbeck & Gegenfurtner, 1998), for which we had determined their subjective isoluminant points at several different temporal frequencies. Details of the procedures used are given in Reisbeck and Gegenfurtner (1998). Since these observers participated in the initial experiments, and since no experimental effect was found under conditions of isoluminance, we simply chose to define isoluminance with respect to the human photopic spectral luminosity function $V(\lambda)$, including Judd's correction, for the other observers (SH, KH and NP).

5.2. Results

Experiment 1 revealed velocity tuning for stimuli defined by luminance contrast. This is indicated by the tilt of the elliptical threshold contours such that the main axes of the contours lie on parallel lines at an orientation of 45° (Fig. 3). Fig. 10 shows the threshold measurements for stimuli defined by isoluminant contrast, together with the best fitting ellipses. As in Fig. 3, a five parameter model for the ellipses provided excellent fits to the observed contours. The mean deviation was 0.7%. In Fig. 10 most of the ellipses are nearly perfectly aligned to the axes of the coordinate system.

Fig. 11 shows this more quantitatively by plotting the angle the orientation of the major axes of the ellipses as a function of standard stimulus velocity. For the isoluminant stimuli, most ellipses are oriented close to 90°, indicating a space–time separable tuning.

Similar results were obtained when we repeated Experiment 3 with isoluminant stimuli. Fig. 12 shows the discrimination thresholds determined either along lines of constant velocity, or along lines of varying velocity, analogous to Fig. 9 for luminance defined stimuli. All the data points fall close to the broken horizontal line, indicating that thresholds under these two conditions were identical.

5.3. Discussion

The results for the isoluminant gratings show that subjects can not use the additional information about

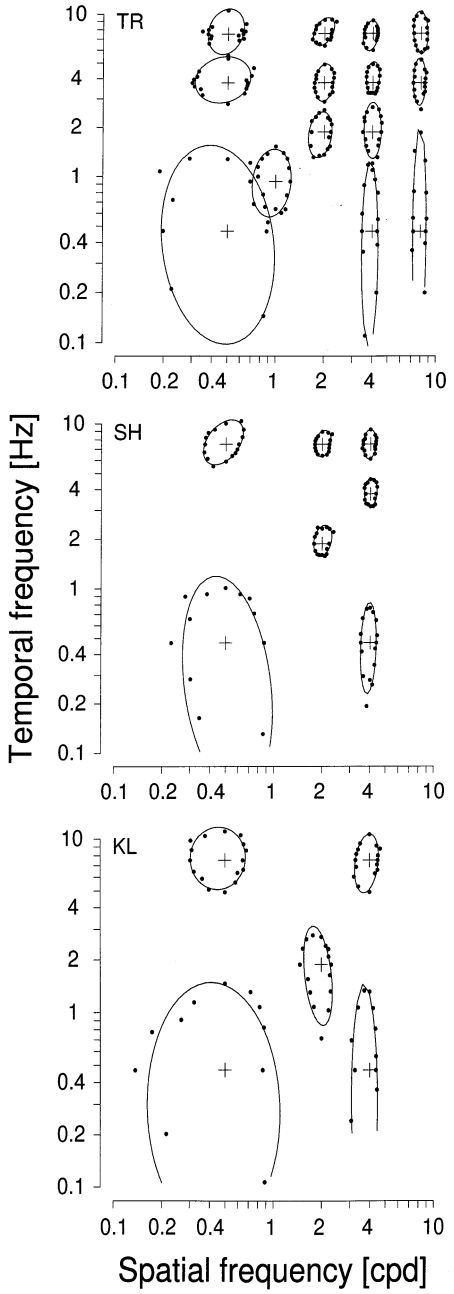

Fig. 10. Threshold contours in the spatio-temporal frequency plane for three observers (TR, SH and KL) using isoluminant stimuli. All other details are given in the figure legend to Fig. 3. In contrast to the results for luminance gratings (Fig. 3) threshold contours are aligned with the coordinate axes. This indicates that discrimination performance is based upon mechanisms that are separably tuned to spatial and temporal frequency and that velocity tuned mechanism do not contribute to discrimination performance.

stimulus velocity in these stimuli to enhance discrimination performance. From this we can conclude that velocity tuned mechanisms either do not exist for isoluminant stimuli, or that their sensitivity is very low. The rms-cone-contrast of the isoluminant stimuli is about one tenth of the contrast of the luminance stimuli,

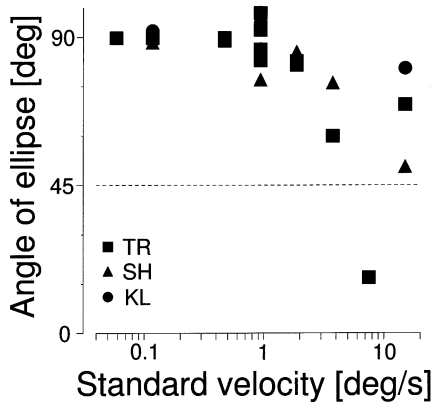

Fig. 11. The orientation of the best fitting ellipses (see Fig. 10) as a function of the velocity of the different isoluminant standard gratings. Subjects are indicated by their initials in the lower left hand corner of the plot. The abscissa represents the velocity of the standard grating on a logarithmic scale, whereas the ordinate indicates the angle of the best fitting ellipses. The broken horizontal line at an orientation of 45° indicates the prediction based upon velocity tuned mechanisms. All data points lie close to 90 or 0°. This indicates that discrimination is primarily based upon separable mechanisms for spatial and temporal frequency.

namely 7.05%. Fig. 9B showed that discrimination performance for stimuli defined by 6.25% luminance contrast was the same for conditions of constant and variable velocity. Contrast can therefore play an essential role in this experiment. However, the contrasts used were at half the maximum possible with our display monitor, and it is hard to imagine why such a mechanism would be useful if its sensitivity was so low. Therefore we can conclude that velocity tuned mechanisms do not contribute significantly to the perception of velocity for isoluminant stimuli.

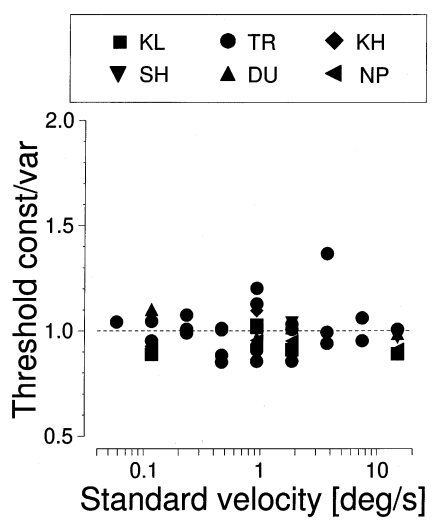

Fig. 12. Ratio of discrimination thresholds for the directions of constant to variable velocity as a function of the velocity of different isoluminant standard gratings. Results are given for the same subjects as in Fig. 9, which displays the results for luminance stimuli. The broken horizontal line predicts the location of the data points if there was no difference in the discrimination performance for the two directions. All symbols cluster along this line thereby indicating that discrimination performance for isoluminant stimuli depends upon separable mechanisms tuned to spatial and temporal frequency. All other details are given in the figure legend to Fig. 9.

In the above experiments, isoluminant stimuli at different spatial frequencies were used. Such stimuli will introduce chromatic aberration and therefore small luminance artifacts (Flitcroft, 1989; Cavanagh & Anstis, 1991; Marimont & Wandell, 1994). Furthermore, the point of isoluminance for a particular observer is known to vary with spatial and temporal frequency (Stromeyer, Chaparro, Tolias & Kronauer, 1995; Gunther, Peterzell & Dobkins, 1998). Even though we determined isoluminance at different temporal frequencies for some of our observers (TR, KL and DU), the presence of small luminance artifacts cannot be excluded. The absence of any discernible velocity tuning at isoluminance simply shows that velocity tuned mechanisms are neither sensitive to chromatic contrast, nor are the able to use any artificial low luminance contrasts (Fig. 9B).

6. General discussion

6.1. Summary

Our results provide direct evidence for the existence of velocity tuned mechanisms in human motion processing. Such mechanisms can add discriminative power to other mechanisms tuned separably to spatial and temporal frequency. Interestingly, the contrast sensitivity of velocity tuned mechanisms seems to be relatively low when compared to separable mechanisms. Furthermore velocity tuned mechanisms seem to be implemented in the luminance domain only. Motion defined by chromatic contrast lacks velocity tuned mechanisms.

6.2. Relationship to other psychophysical experiments

By far the most extensive psychophysical investigation of velocity tuned mechanisms has been the work of McKee et al. (1986). They found that practiced observers could make reliable judgments of velocity discrimination, even though the stimuli had variable temporal frequency and contrast. Observers had to compare the velocity of a set of comparison stimuli to a memorized standard stimulus, identical to the procedure we used in Experiment 3. In their experiment, the spatial and temporal frequency of the comparison stimuli was randomly varied. The resulting Weber fractions for velocity discrimination were only modestly increased from 5 to about 7%. They interpreted the results as evidence that 'temporal frequency is only known indirectly through motion mechanisms whose fundamental dimension is velocity'.

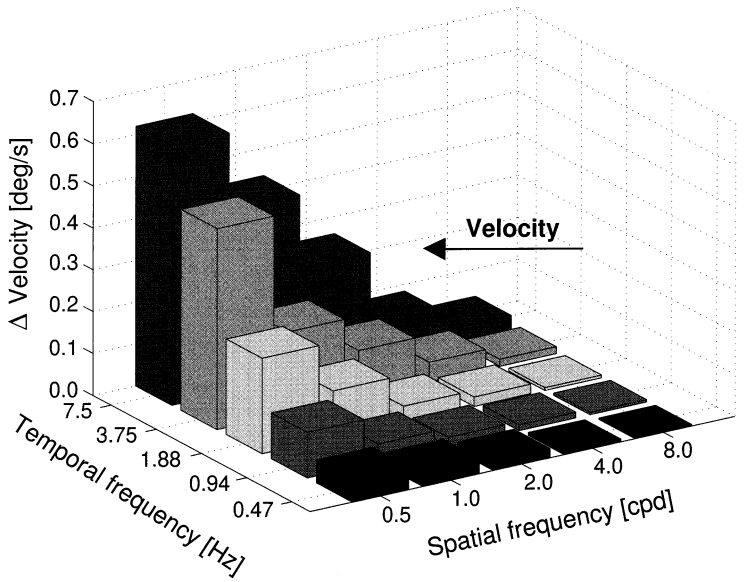

Fig. 13. Velocity differences between 25 standard stimuli and the respective thresholds for the direction of variable velocity. All data from observer TR. Spatial and temporal frequencies are indicated on the abscissas and their intersections specify the standard stimuli for which thresholds have been determined. The ordinate indicates the velocity differences for any of the standard stimuli and the arrow depicts the direction for increasing standard velocities. The highest velocity difference is observed for the highest standard velocity. The differences decrease for increasing spatial and decreasing temporal frequencies producing in each case lower standard velocities. The dependence of the velocity difference at threshold on standard velocity is in accordance with Weber's law.

While these experiments showed that velocity judgments are possible independently of temporal frequency and contrast, they do not conclusively prove the existence of low-level velocity detectors. Rather, what is shown by these results is there is not a *single* temporal frequency selective mechanism that forms the basis of velocity judgments. The results do not rule out the possibility that the elementary detectors are spatio-temporally separable and velocity mediated by a population code of these separable mechanisms. Another basic result of the McKee et al. (1986) study was that velocity discrimination was better than temporal frequency discrimination in terms of lower Weber fractions. This aspect has been challenged recently. Smith and Edgar (1991) and Derrington and Henning (1993) found that with practice Weber fractions for temporal frequency discrimination could be as low or lower than for velocity discrimination. Furthermore, Smith and Edgar (1991) showed, that temporal frequency discrimination was not much affected by random changes in velocity. All these results point to the conclusion that there are indeed three sets of mechanisms tuned to spatial frequency, temporal frequency and velocity, and that the visual system uses all the information available to make reliable and optimal discrimination judgments. This idea is strongly supported by our experiments.

The fact that Weber fractions for velocity discrimination depend on velocity only, and not on spatial and temporal frequency, is also illustrated by the results of Experiment 3. Fig. 13 shows the velocity differences Δv necessary for reliable discrimination at each spatial and temporal frequency. Δv is only dependent on velocity, and the Weber fraction $\Delta v/v$ is relatively constant at around 5%. This could easily be interpreted as evidence for velocity tuned mechanisms underlying this task. However, this is not the case. Exactly the same pattern of thresholds can be produced by spatio-temporally separable mechanisms with constant Weber fractions of 5% for spatial frequency and temporal frequency, respectively.

Using a noise masking paradigm, Burr, Ross and Morrone (1986) also presented evidence for spatio-temporal coupling. However, they measured contrast thresholds for the detection of gratings superimposed with a counterphase flickering masking grating. The spatio-temporal filters reconstructed from these data show nonseparable profiles, but they are not elongated along lines of constant velocity. Rather, the filters have high sensitivity at high spatial and low temporal frequencies, and at low spatial and high temporal frequencies. The filters are therefore responsive over a broad range of velocities, whereas the mechanisms revealed by our experiments integrate over only a small range of velocities. The difference in results is certainly caused by the difference in paradigms. In the Burr et al. (1986) study, only the activity of the most sensitive detectors contributed.

Just recently two very elegant studies have been published that also investigate velocity tuned mechanisms (Schrater & Simoncelli, 1998; Seiffert & Cavanagh, 1998).

Seiffert and Cavanagh (1998) measured for a given temporal frequency the minimum displacement of a grating oscillating in rotational motion. They found that for luminance defined stimuli, the minimum displacement decreased with temporal frequency, thus indicating a velocity criterion for the detection of motion. For second-order, contrast-modulated motion stimuli, the minimum displacement was constant over temporal frequency, indicating position (space–time separable) mechanisms, similar to what we found for isoluminant stimuli. Their results complement ours with respect to low velocity stimuli. Due to the nature of their experiments, Seiffert and Cavanagh (1998) could investigate only stimuli at temporal frequencies of up to 4 Hz, which is the range where our results are ambiguous due to the smear of spatial and temporal frequencies at low spatial and temporal frequencies. While their results indicate velocity tuning for slow velocity stimuli, our results show velocity tuning for stimuli of medium and high velocities.

Schrater and Simoncelli (1998) used an adaptation paradigm to investigate whether adaptation occurs in spatiotemporally separable mechanisms or in velocity tuned mechanisms. They found a spatiotemporal inseparable shift away from the adaptation velocity, supporting the notion of velocity tuned mechanisms.

6.3. Relationship to physiology

Spatially broadband stimuli, such as random dots or bars, are widely used in physiology to address the question of velocity tuning (see, for example, Orban et al., 1981). The drawback of these stimuli is, however, that they can not provide unequivocal evidence concerning the nature of velocity sensitivity. With the use of broadband stimuli alone, it is impossible to decide whether separable mechanisms for spatial and temporal frequency (see Fig. 1A) or velocity tuned mechanisms (Fig. 1B) are realized. For example, the Fourier representation of a random dot stimulus moving at a fixed velocity covers a line of constant velocity through the origin of the spatiotemporal frequency plane, whereas a drifting sinewave grating is represented by a single point on this line. The use of sinewave gratings allows the determination of threshold contours in this plane the shape of which indicates the underlying processing mechanisms (see Experiment 1). However, using spatially broadband random dot stimuli leads to velocity tuning in both cases, whether the underlying filters are velocity tuned or separable.

Fig. 14A shows the hypothetical spatio-temporal frequency tuning profile of two hypothetical mechanisms, one of them separable (dotted contour) and the other one velocity tuned (continuous contour). The peak of both profiles is at a spatial frequency of 4 c/deg and a temporal frequency of 3.75 Hz (cross). The activation profiles of the tuning curves are given by a two-dimensional Gaussian distribution. Both extend equally in spatial and temporal frequency. Fig. 14 B shows the corresponding hypothetical velocity tuning functions obtained with random dot stimuli. The functions were normalized to the cell's maximal response. The dotted

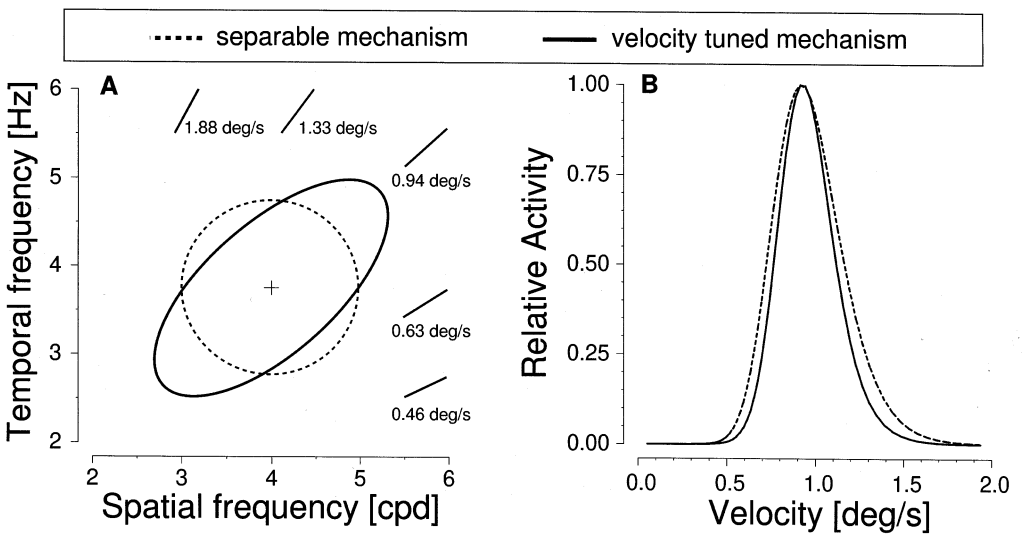

Fig. 14. Model predictions for the velocity tuning for two hypothetical cells with either a separable or a velocity tuned receptive field to random dot stimuli. Plot A shows the separable (broken line) and the velocity tuned (continuous line) receptive field in the plane spanned by spatial and temporal frequency. The cross represents the point of highest activation which declines in a Gaussian like manner towards the edges of the receptive fields. The line segments indicate different velocities. Plot B shows the relative activation of a hypothetical cell for a range of velocities of homogeneously moving random dot fields. The relative activations for a separable and velocity tuned receptive field are given by the broken and the continuous line, respectively. Both tuning functions are almost identical except for the width of the distribution which is slightly broader for the separable receptive field.

line gives the cell's tuning for the separable mechanism and the continuous line the response for the velocity tuned receptive field. The two tuning curves are nearly indistinguishable. The important point is that on the basis of these velocity tuning functions no information can be obtained whether the underlying mechanisms are separable or tuned to velocity. This restriction can be overcome by the use of sinewave gratings which allow a direct test of the nature of these mechanisms.

There have been only few physiological experiments in which sinewave gratings were used to address the issue of velocity tuned versus separable mechanisms. Levitt et al. (1994) and Foster et al. (1985) both showed that receptive fields for most single neurons in area V2 are spatio-temporally separable. It has long been hypothesized that neurons in area MT would show velocity tuning. The only data so far testing this idea critically have only been published in abstract form (Newsome et al., 1983; Movshon et al., 1988) and support the notion that the majority of MT neurons is spatiotemporally separable.

6.4. Stimulus contrast

The results of Experiment 3 showed that contrast has a profound influence on the discrimination performance of our subjects (see Fig. 9B). Under conditions of low (6.25%) stimulus contrast subjects could not use the additional information about stimulus velocity to achieve lower discrimination thresholds as compared to stimuli that differ only in spatial and temporal frequency from the standard grating. What is intriguing, however, is the fact that thresholds remained the same with respect to spatial frequency at both contrast levels. Only the velocity tuned mechanisms were affected by the reduction in contrast, and not the spatio-temporally separable mechanisms. This finding is at odds with our earlier speculations about the location where velocity information might be processed. MT neurons have high contrast sensitivity (Albright, 1984; Sclar et al., 1990) and we would therefore expect that a reduction in stimulus contrast would produce little effect in our data. Therefore the current results point to the possibility that velocity is extracted at a stage of the motion pathway that is situated higher than MT. Other results on the contrast dependence of perceived velocity for contrasts of 50% and higher support this notion.

6.5. Color and motion

The results for isoluminant stimuli showed that the discrimination of test against standard stimuli depended in a separable manner on spatial and temporal frequency. This holds for the results of Experiment 1 where we determined threshold contours as well as for Experiment 3 where psychometric functions were obtained under conditions of best discriminability. In both experiments, velocity components of the test stimuli could not be used by our subjects to enhance discrimination performance. This is in agreement with a large number of earlier psychophysical results showing that perception of velocity is impaired under conditions of isoluminance (Cavanagh et al., 1984; Mullen & Boulton, 1992; Teller & Lindsey, 1993; Hawken et al., 1994; Gegenfurtner & Hawken, 1996a), even though directional sensitivity is excellent under those conditions (Stromeyer et al., 1990; Cavanagh & Anstis 1991; Fiorentini, Burr & Morrone, 1991; Derrington & Henning, 1993; Metha et al., 1994; Stromeyer et al., 1995; Gegenfurtner & Hawken, 1996b).

Acknowledgements

We are grateful to Mike Hawken for commenting on an earlier version of this manuscript. We would like to thank the two anonymous reviewers for their helpful suggestions. K. R. Gegenfurtner was supported by a Heisenberg-Fellowship from the German Research Council (DFG Ge 879/4-1).

References

Adelson, E. H., & Bergen, J. R. (1985). Spatiotemporal energy models for the perception of motion. *Journal of the Optical Society of America A*, *2*, 284–299.

Albright, T. D. (1984). Direction and orientation selectivity of neurons in visual area MT of the macaque. *Journal of Neurophysiology*, *52*, 1106–1130.

Bisti, S., Carmignoto, G., Galli, L., & Maffei, L. (1985). Spatial-frequency characteristics of neurones of area 18 in the cat: dependence on the velocity of the visual stimulus. *Journal of Physiology*, *359*, 259–268.

Brainard, D. (1989). Calibration of a computer controlled color monitor. *Color Research and Application*, *14*, 23–34.

Britten, K. H., Shadlen, M. N., Newsome, W. T., & Movshon, J. A. (1992a). Responses of neurons in macaque MT to stochastic motion signals. *Visual Neuroscience*, *10*, 1157–1169.

Britten, K. H., Shadlen, M. N., Newsome, W. T., & Movshon, J. A. (1992b). The analysis of visual motion: a comparison of neuronal and psychophysical performance. *Journal of Neuroscience*, *12*, 4745–4765.

Britten, K. H., Newsome, W. T., Shadlen, M. N., Celebrini, S., & Movshon, J. A. (1996). A relationship between behavioral choice and the visual responses of neurons in macaque MT. *Visual Neuroscience*, *13*, 87–100.

Burkhalter, A., & Van Essen, D. C. (1986). Processing of color, form, and disparity information in visual areas VP and V2 in ventral extrastriate cortex in macaque monkey. *Journal of Neuroscience*, *6*, 2327–2351.

Burr, D. C., Ross, J., & Morrone, M. C. (1986)). Seeing objects in motion. *Proceedings of the Royal Society of London B*, *227*, 249–265.

Campbell, F. W., Cleland, B. G., Cooper, G. F., & Enroth-Cugell, C. (1968). The angular selectivity of visual cortical cells to moving gratings. *Journal of Physiology*, *198*, 237–250.

Campbell, F. W., Cooper, G. F., & Enroth-Cugell, C. (1969). The spatial selectivity of the visual cells of the cat. *Journal of Physiology*, *203*, 223–235.

Cavanagh, P., Tyler, C. W., & Favreau, O. (1984). Perceived velocity of moving chromatic gratings. *Journal of the Optical Society of America A*, *1*, 893–899.

Cavanagh, P., & Anstis, S. (1991). The contribution of color to motion in normal and color-deficient observers. *Vision Research*, *31*, 2109–2148.

D'Zmura, M. (1990). *Surface color psychophysics*. Ph.D. Dissertation, University of Rochester, Rochester, NY.

DeBruyn, B., & Orban, G. A. (1988). Human velocity and direction discrimination measured with random dot patterns. *Vision Research*, *28*, 1323–1335.

De Valois, R. L., Albrecht, D. G., & Thorell, L. G. (1982). Spatial frequency selectivity of cells in macaque visual cortex. *Vision Research*, *22*, 545–559.

De Valois, R. L., & De Valois, K. K. (1988). *Spatial vision*. *Oxford psychology series 14*. Oxford: Oxford University.

Derrington, A. M., & Henning, G. B. (1989). Some observations on the masking effects of two-dimensional stimuli. *Vision Research*, *29*, 241–246.

Derrington, A. M., & Henning, G. B. (1993). Detecting and discriminating the direction of motion of luminance and colour gratings. *Vision Research*, *33*, 799–811.

Dow, B. M. (1974). Functional classes of cells and their laminar distribution in monkey visual cortex. *Journal of Neurophysiology*, *37*, 927–946.

Dubner, R., & Zeki, S. M. (1971). Response properties and receptive fields of cells in an anatomically defined region of the superior temporal sulcus in the monkey. *Brain Research*, *35*, 528–532.

Fiorentini, A., Burr, D. C., & Morrone, C. M. (1991). Temporal characteristics of colour vision: VEP and psychophysical measurements. In A. Valberg, & B. B. Lee, *From pigments to perception* (pp. 139–149). New York: Plenum.

Flitcroft, D. I. (1989). The interactions between chromatic aberration, defocus and stimulus chromaticity: implications for visual physiology and colorimetry. *Vision Research*, *29*, 349–360.

Foster, K. H., Gaska, J. P., Nagler, M., & Pollen, D. A. (1985). Spatial and temporal frequency selectivity of neurones in visual cortical areas V1 and V2 of the macaque monkey. *Journal of Physiology*, *365*, 331–363.

Gegenfurtner, K. R., & Kiper, D. C. (1992). Contrast detection in luminance and chromatic noise. *Journal of the Optical Society of America A*, *9*, 1880–1888.

Gegenfurtner, K. R., & Hawken, M. J. (1995). Temporal and chromatic properties of motion mechanisms. *Vision Research*, *35*, 1547–1563.

Gegenfurtner, K. R., & Hawken, M. J. (1996a). Perceived speed of luminance, chromatic and non-Fourier stimuli: influence of contrast and temporal frequency. *Vision Research*, *36*, 1281–1290.

Gegenfurtner, K. R., & Hawken, M. J. (1996b). Interactions of color and motion in the visual pathways. *Trends in Neuroscience*, *19*, 394–401.

Grzywacz, N. M., & Yuille, A. L. (1990). A model for the estimate of local image velocity by cells in the visual cortex. *Proceedings of the Royal Society of London B*, *239*, 129–161.

Gunther, K. L., Peterzell, D. H., & Dobkins, K. R. (1998). Are red/green isoluminance matches served by the same spatiotemporal covariance mechanisms that underlie chromatic and luminance contrast sensitivity? *Investigative Ophthalmology and Visual Science* (*Suppl.*), *39*, 1078.

Hawken, M. J., Parker, A. J., & Lund, J. S. (1988). Laminar organization and contrast sensitivity of direction-selective cells in the striate cortex of the old world monkey. *Journal of Neuroscience*, *8*, 3541–3548.

Hawken, M. J., Gegenfurtner, K. R., & Tang, C. (1994). Contrast dependence of colour and luminance motion mechanisms in human vision. *Nature*, *367*, 268–270.

Heeger, D. J. (1987). Model for the extraction of image flow. *Journal of the Optical Society of America A*, *4*, 1455–1471.

Heeger, D. J., Simoncelli, E. P., & Movshon, J. A. (1996). Computational models of cortical visual processing. *Proceedings of the National Academy of Science USA*, *93*, 623–627.

Henning, G. B., Hertz, B. G., & Hinton, J. L. (1981). Effects of different hypothetical detection mechanisms on the shape of spatial-frequency filters inferred from masking experiments: I. Noise masks. *Journal of the Optical Society of America*, *71*, 574–581.

Holub, R. A., & Morton-Gibson, M. (1981). Response of visual cortical neurons of the cat to moving sinusoidal gratings: response-contrast functions and spatiotemporal interactions. *Journal of Neurophysiology*, *46*, 1244–1259.

Hubel, D. H., & Wiesel, T. N. (1962). Receptive fields, binocular interaction, and functional architecture in the cat's visual cortex. *Journal of Physiology*, *160*, 106–154.

Hubel, D. H., & Wiesel, T. N. (1968). Receptive fields and functional architecture of monkey striate cortex. *Journal of Physiology*, *195*, 215–243.

Ikeda, H., & Wright, M. J. (1975). Spatial and temporal properties of 'sustained' and 'transient' neurones in area 17 of the cat's visual cortex. *Experimental Brain Research*, *22*, 363–383.

Irtel, H. (1992). Computing data for color-vision modeling. *Behavior Research Methods*, *Instruments & Computers*, *24*, 397–401.

Krauskopf, J., Williams, D. R., & Heeley, D. W. (1982)). Cardinal directions of color space. *Vision Research*, *22*, 1123–1131.

Krauskopf, J., & Gegenfurtner, K. R. (1992). Color discrimination and adaptation. *Vision Research*, *32*, 2165–2175.

Legge, G. E., Kersten, D., & Burgess, A. E. (1987). Contrast discrimination in noise. *Journal of the Optical Society of America A*, *4*, 391–404.

Levitt, H. (1971). Transformed up-down methods in psychoacoustics. *Journal of the Acoustical Society of America*, *49*, 467–477.

Levitt, J. B., Kiper, D. C., & Movshon, J. A. (1994). Receptive fields and functional architecture of macaque V2. *Journal of Neurophysiology*, *71*, 2517–2542.

Livingstone, M. S., & Hubel, D. H. (1984). Anatomy and physiology of a color system in the primate visual cortex. *Journal of Neuroscience*, *4*, 309–356.

Livingstone, M. S., & Hubel, D. H. (1987). Psychophysical evidence for separate channels for the perception of form, color, movement and depth. *Journal of Neuroscience*, *7*, 3416–3468.

Losada, M. A., & Mullen, K. T. (1994). The spatial tuning of chromatic mechanisms identified by simultaneous masking. *Vision Research*, *34*, 331–341.

Losada, M. A., & Mullen, K. T. (1995). Color and luminance spatial tuning estimated by noise masking in the absence of off-frequency locking. *Journal of the Optical Society of America A*, *12*, 250–260.

MacLeod, D. I. A., & Boynton, R. M. (1979)). Chromaticity diagram showing cone excitation by stimuli of equal luminance. *Journal of the Optical Society of America*, *69*, 1183–1186.

Marimont, D., & Wandell, B. A. (1994). Matching color images: the effects of axial chromatic aberration. *Journal of the Optical Society of America A*, *11*, 3113–3122.

Maunsell, J. H. R., & Van Essen, D. C. (1983). Functional properties of neurons in middle temporal visual area of the macaque monkey. I. Selectivity for stimulus direction, speed, and orientation. *Journal of Neurophysiology*, *49*, 1127–1147.

McKee, S. P. (1981). A local mechanism for differential velocity detection. *Vision Research*, *21*, 491–500.

McKee, S. P., & Nakayama, K. (1984). The detection of motion in the peripheral visual field. *Vision Research*, *24*, 25–32.

McKee, S. P., Silverman, G. H., & Nakayama, K. (1986). Precise velocity discrimination despite random variations in temporal frequency and contrast. *Vision Research*, *26*, 609–616.

Metha, A. B., Vingrys, A. J., & Badcock, D. R. (1994). Detection and discrimination of moving stimuli: the effects of color, luminance, and eccentricity. *Journal of the Optical Society of America A*, *11*, 1697–1709.

Morrone, M. C., Di Stefano, M., & Burr, D. C. (1986). Spatial and temporal properties of neurons of the lateral suprasylvian cortex of the cat. *Journal of Neurophysiology*, *56*, 969–986.

Movshon, J. A. (1975). The velocity tuning of single units in cat striate cortex. *Journal of Physiology*, *249*, 445–468.

Movshon, J. A., Thompson, I. D., & Tolhurst, D. J. (1978a). Receptive field organization of complex cells in the cat's striate cortex. *Journal of Physiology*, *283*, 79–99.

Movshon, J. A., Thompson, I. D., & Tolhurst, D. J. (1978b). Spatial summation in the receptive fields of simple cells in the cat's striate cortex. *Journal of Physiology*, *283*, 53–77.

Movshon, J. A., Thompson, I. D., & Tolhurst, D. J. (1978c). Spatial and temporal contrast sensitivity of neurones in areas 17 and 18 of the cat's visual cortex. *Journal of Physiology*, *283*, 101–120.

Movshon, J. A., Newsome, W. T., Gizzi, M. S., & Levitt, J. B. (1988). Spatio-temporal tuning and speed sensitivity in macaque visual cortical neurons. *Investigative Ophthalmology and Visual Science* (*Suppl.*), *29*, 327.

Mullen, K. T., & Boulton, J. C. (1992). Interactions between colour and luminance contrast in the perception of motion. *Ophthalmic & Physiological Optics*, *12*, 201–205.

Nakayama, K., & Silverman, G. H. (1984). Temporal and spatial characteristics of the upper displacement limit for motion in random dots. *Vision Research*, *24*, 293–299.

Newsome, W. T., Gizzi, M. S., & Movshon, J. A. (1983). Spatial and temporal properties of neurons in macaque MT. *Investigative Ophthalmology and Visual Science* (*Suppl.*), *24*, 106.

Newsome, W. T., Britten, K. H., & Movshon, J. A. (1989). Neuronal correlates of a perceptual decision. *Nature*, *341*, 52–54.

Newsome, W. T., Britten, K. H., Salzman, C. D., & Movshon, J. A. (1990). Neuronal mechanisms of motion perception. *Cold Spring Harbor Symposia on Quantitative Biology*, *55*, 697–705.

Newsome, W. T. (1997). The King Solomon lectures in neuroethology. Deciding about motion: linking perception to action. *Journal of Comparative Physiology A—Sensory Neural & Behavioral Physiology*, *181*, 5–12.

Nielsen, K. R., & Wandell, B. A. (1988). Discrete analysis of spatial-sensitivity models. *Journal of the Optical Society of America A*, *5*, 743–755.

Orban, G. A., Kennedy, H., & Maes, H. (1981). Response to movement of neurons in areas 17 and 18 of the cat: velocity sensitivity. *Journal of Neurophysiology*, *45*, 1043–1058.

Orban, G. A., De Wolf, J., & Maes, H. (1984). Factors influencing velocity coding in the human visual system. *Vision Research*, *24*, 33–39.

Orban, G. A., Kennedy, H., & Bullier, J. (1986). Velocity sensitivity and direction selectivity of neurons in areas V1 and V2 of the monkey: influence of eccentricity. *Journal of Neurophysiology*, *56*, 462–480.

Pelli, D. (1981). *The effects of visual noise*. Ph.D. Dissertation, Cambridge University, Cambridge.

Poirson, A. B., Wandell, B. A., Varner, D. C., & Brainard, D. H. (1990). Surface characterizations of color thresholds. *Journal of the Optical Society of America A*, *7*, 783–789.

Reichardt, W. (1961). Autocorrelation, a principle for the evaluation of sensory information by the central nervous system. In W. Rosenblith, *Sensory communication*. New York: Wiley.

Reisbeck, T. E., & Gegenfurtner, K. R. (1997). Velocity tuned mechanisms in human motion perception. *Investigative Ophthalmology and Visual Science* (*Suppl.*), *38*, 376.

Reisbeck, T. E., & Gegenfurtner, K. R. (1998). Effects of contrast and temporal frequency on orientation discrimination for luminance and isoluminant stimuli. *Vision Research*, *38*, 1105–1117.

Salzman, C. D., Britten, K. H., & Newsome, W. T. (1990). Cortical microstimulation influences perceptual judgements of motion direction. *Nature*, *346*, 174–177.

Salzman, C. D., Murasugi, C. M., Britten, K. H., & Newsome, W. T. (1992). Microstimulation in visual area MT: effects on direction discrimination performance. *Journal of Neuroscience*, *12*, 2331–2355.

Sankeralli, M. J., & Mullen, K. T. (1997). Postreceptoral chromatic detection mechanisms revealed by noise masking in three-dimensional cone contrast space. *Journal of the Optical Society of America A*, *14*, 2633–2646.

Schrater, P. R., & Simoncelli, E. P. (1998). Local velocity representation: evidence from motion adaptation. *Vision Research*, *38*, 3899–3912.

Sclar, G., Maunsell, J. H., & Lennie, P. (1990). Coding of image contrast in central visual pathways of the macaque monkey. *Vision Research*, *30*, 1–10.

Seiffert, A. E., & Cavanagh, P. (1998). Position displacement, not velocity, is the cue to motion detection of second-order stimuli. *Vision Research*, *38*, 3569–3582.

Simoncelli, E. P., & Heeger, D. J. (1998). A model of neural responses in visual area MT. *Vision Research*, *38*, 743–761.

Smith, A. T., & Edgar, G. K. (1991)). The separability of temporal frequency and velocity. *Vision Research*, *31*, 321–326.

Smith, A. T., & Edgar, G. K. (1994). Antagonistic comparison of temporal frequency filter outputs as a basis for speed perception. *Vision Research*, *34*, 253–265.

Smith, V. C., & Pokorny, J. (1975). Spectral sensitivity of the foveal cone photopigments between 400 and 500 nm. *Vision Research*, *15*, 161–171.

Snowden, R. J., & Braddick, O. J. (1991). The temporal integration and resolution of velocity signals. *Vision Research*, *31*, 907–914.

Stone, L. S., & Thompson, P. (1992). Human speed perception is contrast dependent. *Vision Research*, *32*, 1535–1549.

Stromeyer, C. F. III, Eskew, R. T., & Kronauer, R. E. (1990). The most sensitive motion detectors in humans are spectrally opponent. *Investigative Ophthalmology and Visual Science* (*Suppl.*), *31*, 240.

Stromeyer, C. F. III, Kronauer, R. E., Ryu, A., Chaparro, A., & Eskew, R. T. (1995). Contributions of human long-wave and middle-wave cones to motion detection. *Journal of Physiology*, *485.1*, 221–243.

Stromeyer, C. F. III, Chaparro, A., Tolias, A., & Kronauer, R. E. (1995). Equiluminant settings change markedly with temporal frequency. *Investigative Ophthalmology and Visual Science* (*Suppl.*), *36*, 210.

Switkes, E., Bradley, A., & De Valois, K. K. (1988). Contrast dependence and mechanisms of masking interactions among chromatic and luminance gratings. *Journal of the Optical Society of America A*, *5*, 1149–1162.

Teller, D. Y., & Lindsey, D. T. (1993). Motion at isoluminance: motion dead zones in three-dimensional color space. *Journal of the Optical Society of America A*, *10*, 1324–1331.

Thompson, P. (1982). Perceived rate of movement depends on contrast. *Vision Research*, *22*, 377–380.

Tolhurst, D. J., & Movshon, J. A. (1975). Spatial and temporal contrast sensitivity of striate cortical neurones. *Nature*, *257*, 674–675.

Van Santen, J. P. H., & Sperling, G. (1984). A temporal covariance model of motion perception. *Journal of the Optical Society of America A*, *1*, 451–473.

Watson, A. B., & Ahumada, A. J. (1985). Model of human visual-motion sensing. *Journal of the Optical Society of America*, *2*, 322–341.

Wilson, H. R., McFarlane, D. K., & Phillips, G. C. (1983). Spatial frequency tuning of orientation selective units estimated by oblique masking. *Vision Research*, *23*, 873–882.